Supplementary Materials

Manipulating surface buffer of transition metal sulfide for robust seawater electrolysis

Shijia Cheng[1,2], Siyuan Tang[1,*], Xiang Ding[1], Nan Jiang[3,*], Haotian Qin[1], Yin Yin[1,*], Fuzhan Song[1,*]

[1]School of Materials Science and Engineering, Jiangsu University, Zhenjiang 212013, Jiangsu, China.

[2]Nanyang Technological University, 50 Nanyang Avenue, Singapore 639798, Singapore.

[3]Department of Chemistry and Chemical Engineering, Guizhou University, Guiyang 550025, Guizhou, China.

[*]**Correspondence to:** Dr. Siyuan Tang, Prof. Fuzhan Song, Prof. Yin Yin, School of Materials Science and Engineering, Jiangsu University, Zhenjiang 212013, Jiangsu, China. E-mail: 2112305054@stmail.ujs.edu.cn; fzsong@ujs.edu.cn; yyin@ujs.edu.cn; Prof. Nan Jiang, Department of Chemistry and Chemical Engineering, Guizhou University, Guiyang 550025, Guizhou, China. E-mail: njiang@gzu.edu.cn

1. Chemicals

All commercial chemicals were used as received without any further purification. Ammonium chloride (NH_4Cl, 95%, Aladdin), Nickel chloride ($NiCl_2·6H_2O$, 99.4%, Aladdin), Chromium chloride ($CrCl_3·6H_2O$, 99%, Aladdin), Potassium hydroxide (KOH, 85%, Alfa Aesar), Thiourea (CH_4N_2S, AR, Sigma-Aldrich) and Sulfur (S, AR, Sigma-Aldrich) were purchased from Fisher Chemical. Anhydrous acetonitrile (CH_3CN, 99.95%, Alfa Aesar) was purchased from Pharmco. All water was deionized (18 MΩ×cm) with a Barnstead E-Pure system in all experiments.

2. Characterization

Scanning electron microscopy (SEM) measurement and elemental mapping analysis were conducted on an FEI Quanta 650 FEG microscope equipped with an INCA 350 spectrometer (Oxford Instruments) for energy dispersive X-ray (EDX) spectroscopy. Transmission electron microscopy (TEM) measurement was carried out on an FEI Tecnai G2 F20 FE-TEM (FEI, USA). X-ray diffraction (XRD) patterns were obtained on a Rigaku MinifexII Desktop X-ray diffractometer. The X-ray photoelectron spectroscopy (XPS) measurements were performed using a Kratos Axis Ultra instrument (Kratos Analytical Ltd.).

3. Experimental

3.1 Syntheses of Pt/C

The commercial 20 wt % Pt/C samples were prepared by ultrasonically mixing 5.6 mg of the catalyst powder with the mixture of 900 μL of ethanol, 580 μL of H_2O, and 120 μL of a 5% Nafion solution for 1 h to form homogeneous catalyst inks. Then, the ink was dropped on NF and the Pt/C load was 4.0 mg cm^{-2}.

3.2 Electrochemical measurement

All electrochemical performance was measured using a Gamry Interface 1000 electrochemical workstation. The current densities in this work were calculated on the basis of the geometric area of each working electrode.

The obtained NiCrS@CN was directly used as the working electrode. A calibrated Hg/HgCl (saturated KCl) with a salt bridge kit and a carbon rod were used as the counter and reference electrode, respectively. The electrolytes for HER/OER was 1.0 M KOH. H_2 was bubbled through all electrolytes used during each electrochemical experiment.

All HER measurements in alkaline seawater and freshwater are conducted in the same configuration. The alkaline seawater electrolyte was prepared by dissolving KOH in natural seawater to obtain a concentration of 1 M seawater, with the same KOH concentration and pH value as the alkaline freshwater electrolyte. For both seawater electrocatalysis and freshwater electrocatalysis, a calibrated Hg/HgCl (saturated KCl) with a salt bridge kit and a carbon rod were used as the counter and reference electrode, respectively. To avoid any potential cross-contamination or electrode effects, a fresh working electrode was used for each electrolyte system.

All potentials are reported versus reversible hydrogen electrode (RHE) according to the following equation:

$$E\ (vs.\ RHE) = E\ (vs.\ Hg/HgCl) + 0.241 + 0.059 \times pH \qquad (S1)$$

Linear sweep voltammetry (LSV)

All polarization curves were recorded using linear scan voltammetry (LSV). The scan rate was 5 mV/s. Unless otherwise stated, all LSV curves for HER were iR corrected and obtained by scanning from a negative to positive potential. A correction was made according to the following equation:

$$E_{corrected} = E_{measured} - iR_s \qquad (S2)$$

where $E_{corrected}$ is the iR-corrected potential, $E_{measured}$ and i are experimentally measured potential and current, respectively, and R_s is the equivalent series resistance measured via electrochemical impedance spectroscopy. Tafel plots were constructed using the equation:

$$\eta = a + b \log|j| \qquad (S3)$$

where η is the overpotential, a is the intercept, b is the Tafel slope, and j is the current density.

Electrochemical impedance spectroscopy (EIS)

Electrochemical impedance spectroscopy (EIS) measurements in 1.0 M KOH were

carried out at -0.083 V vs RHE for HER and 1.517 V vs RHE for OER in the frequency range of 10^6 – 0.01 Hz.

Electrochemically active surface area (ECSA)

The electrochemically active surface area (ECSA) of each working electrode was determined according to an established methodology reported in the literature. CV cycling was repeated using a range of scan rates from 20 to 100 mV s^{-1}. The electrochemical double-layer capacitance (C_{dl}) was then estimated by plotting the difference between the anodic and cathodic current densities ($\Delta j = j_a - j_c$) at OCP against the scan rate. The resulting linear slope is twice of the C_{dl}. The ESCA can be calculated according to the following equation: $ECSA = C_{dl} / C_s$, where Cs is the specific capacitance of a flat smooth surface of the electrode material, according to the literature.

Chronopotentiometry (CP)

The catalytic stability was evaluated by CP measurement with iR correction.

For overall water splitting, a symmetrical full electrolyzer was constructed using NiCrS@CN as anode and cathode. Overall water splitting performance was evaluated using LSV and CP in a two-electrode configuration in 1.0 M KOH. LSV curves were recorded at a sweep rate of 5 mV s^{-1}.

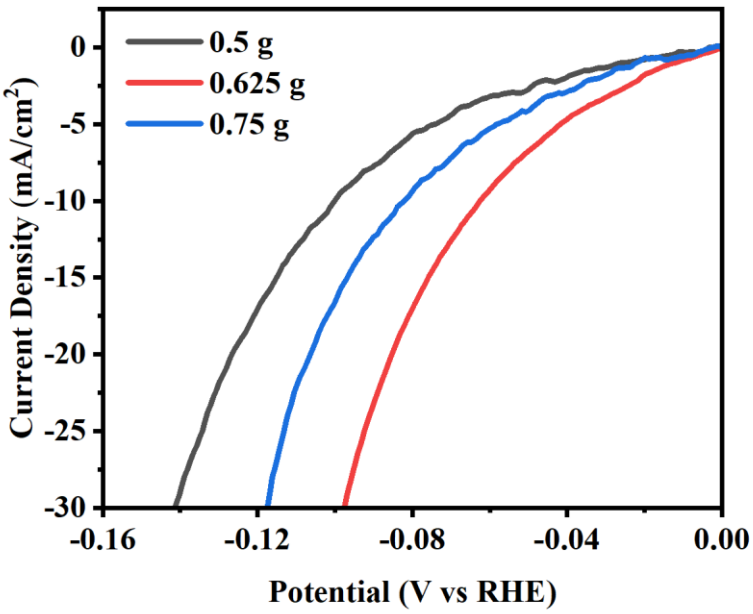

Figure S1. HER polarization curves of NiCrS/CN under different thiourea amounts

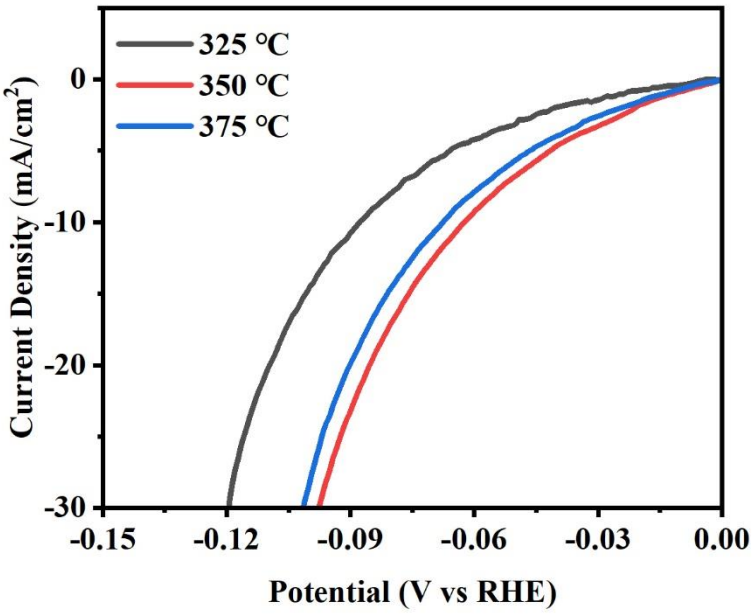

Figure S2. HER polarization curves of NiCrS/CN at different temperatures

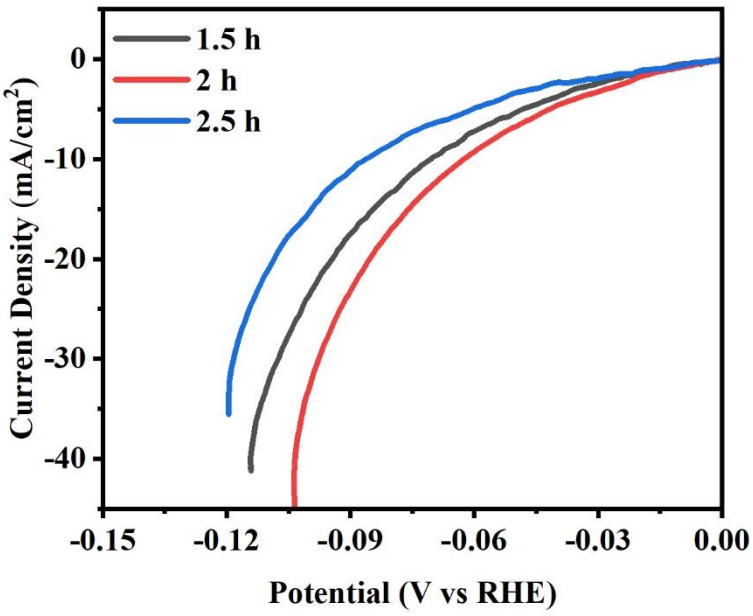

Figure S3. HER polarization curves of NiCrS/CN under different times

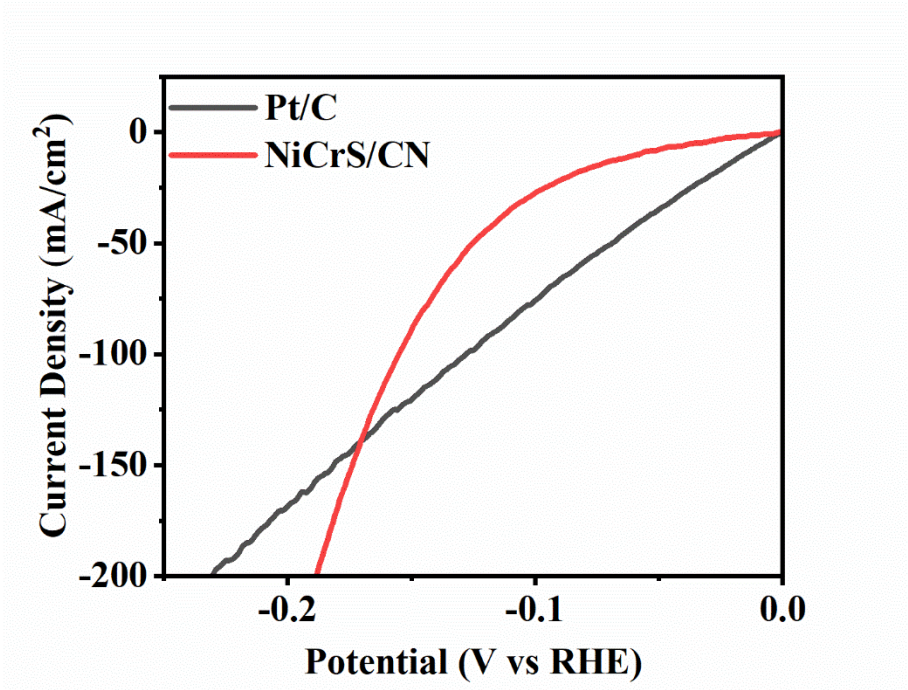

Figure S4. HER polarization curves of NiCrS/CN and Pt/C

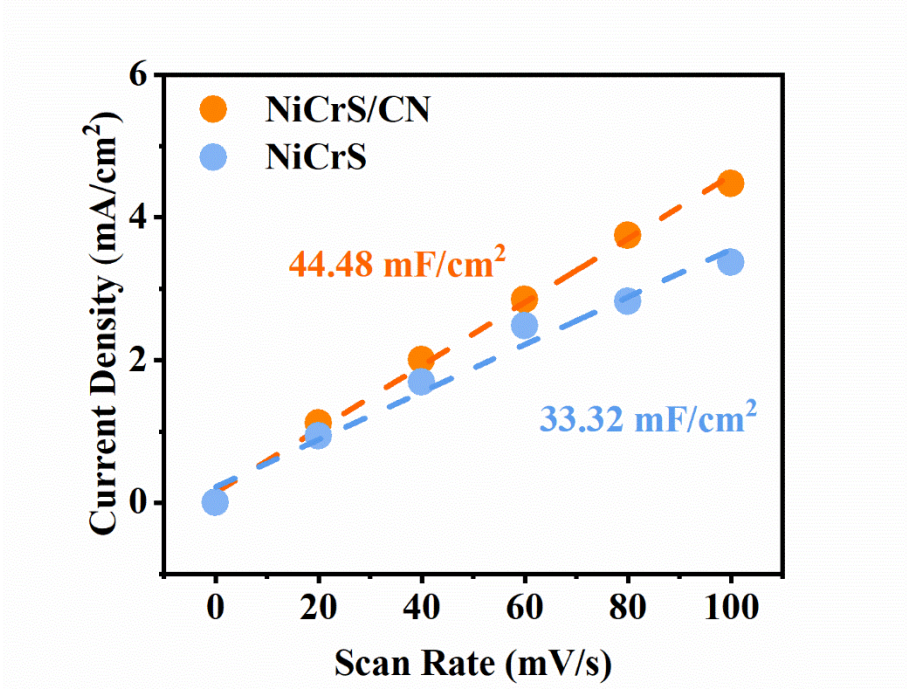

Figure S5. ECSA of NiCrS and NiCrS/CN

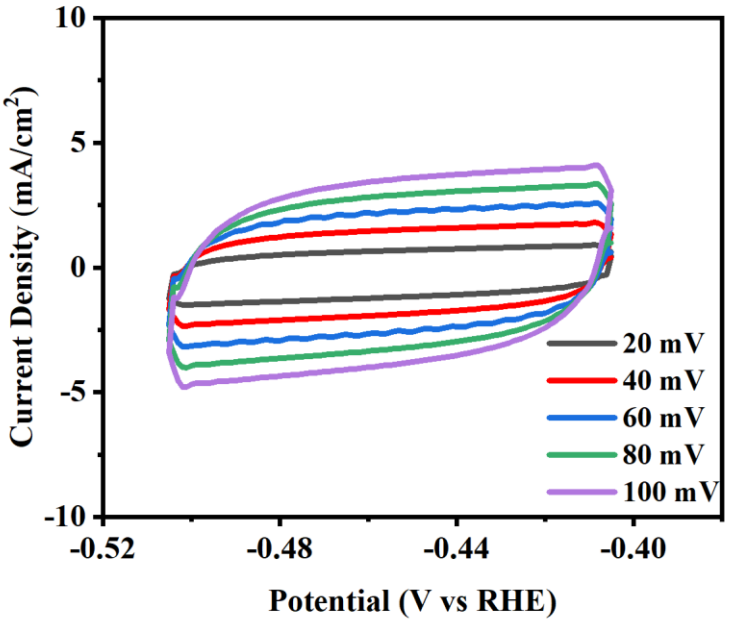

Figure S6. C_{dl} of NiCrS

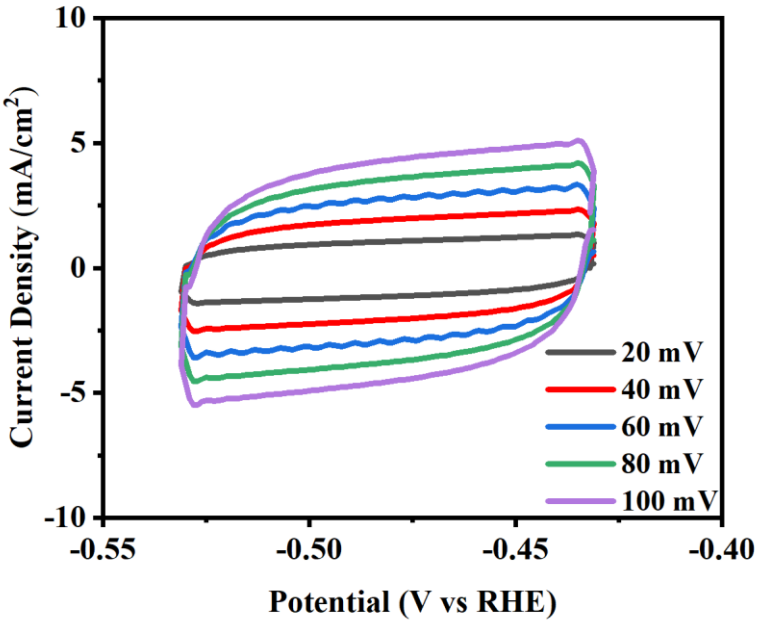

Figure S7. C_{dl} of NiCrS@CN

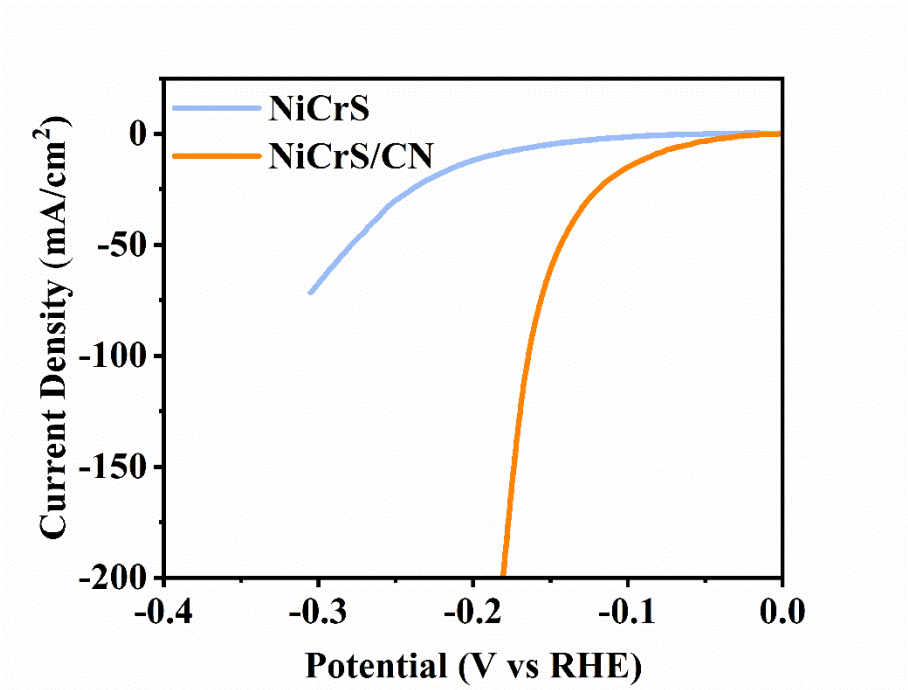

Figure S8. HER polarization curves of NiCrS/CN and NiCrS in 1 M KOH + Seawater

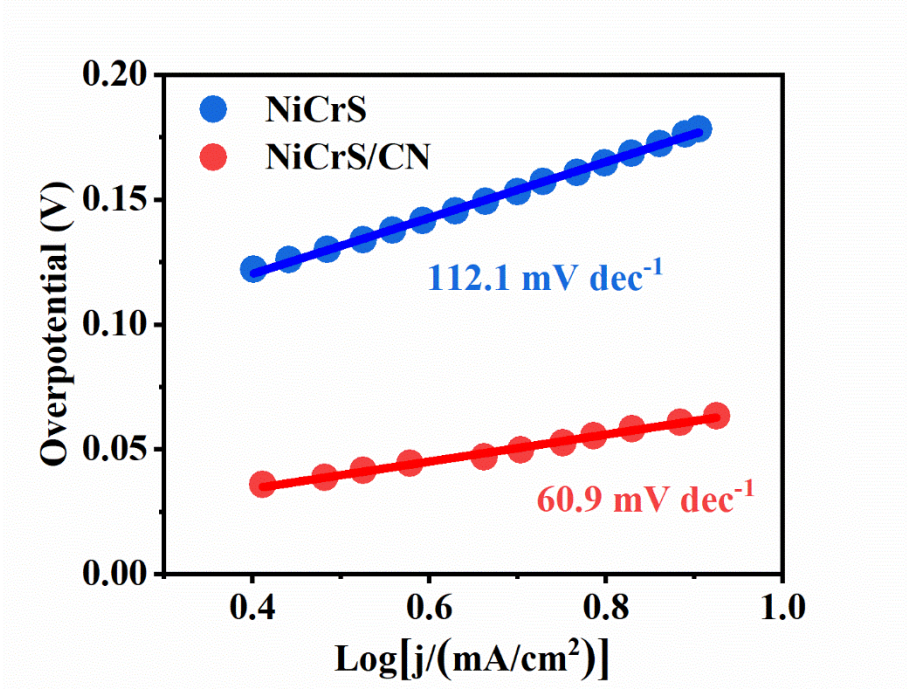

Figure S9. Tafel plots of NiCrS and NiCrS/CN in 1 M KOH + Seawater

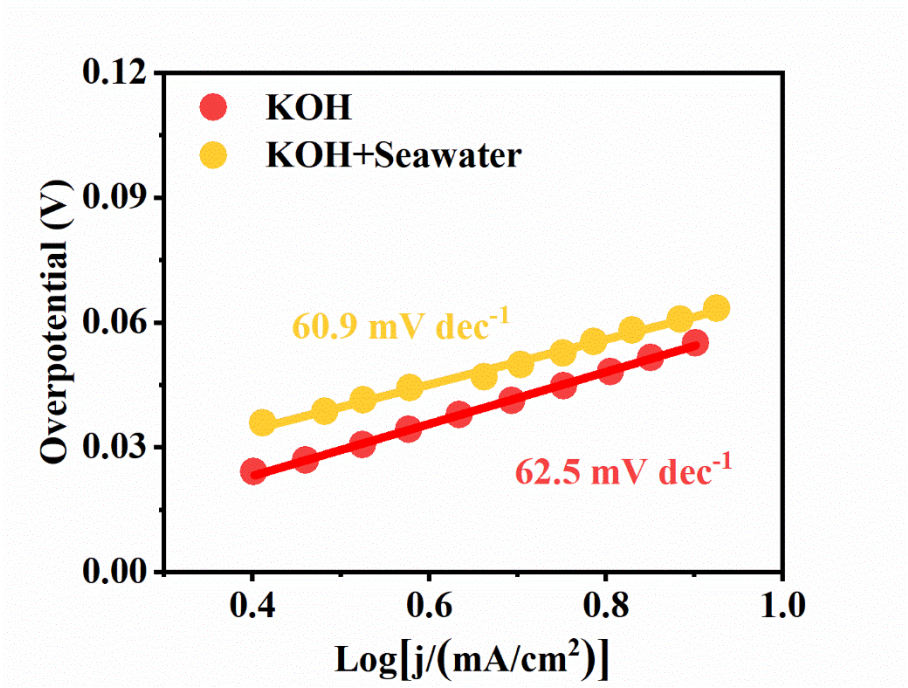

Figure S10. Tafel plots of NiCrS/CN in 1 M KOH and 1 M KOH + Seawater

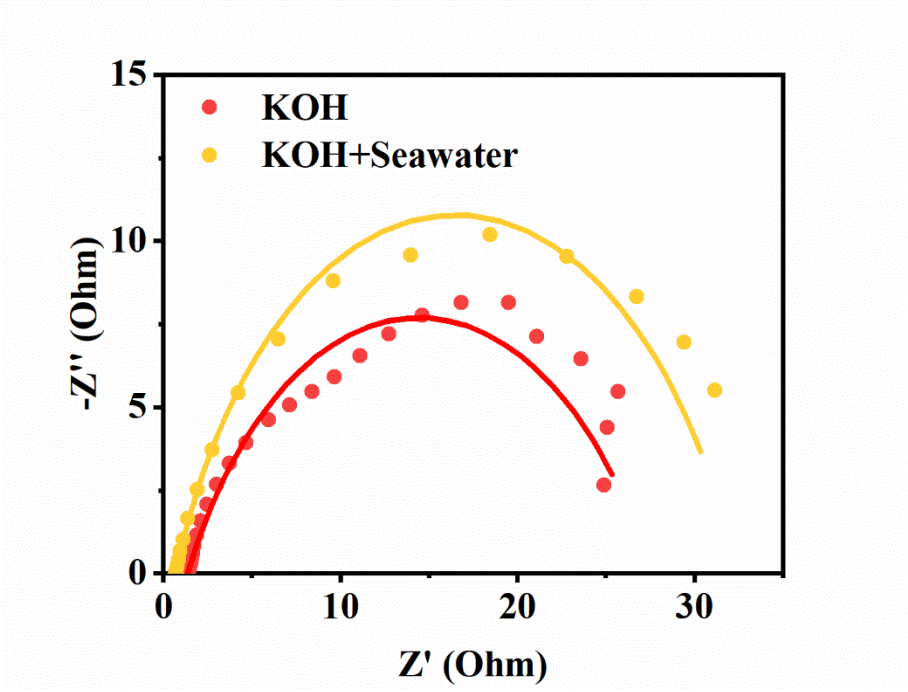

Figure S11. Nyquist diagram of NiCrS/CN in 1 M KOH and 1 M KOH + Seawater

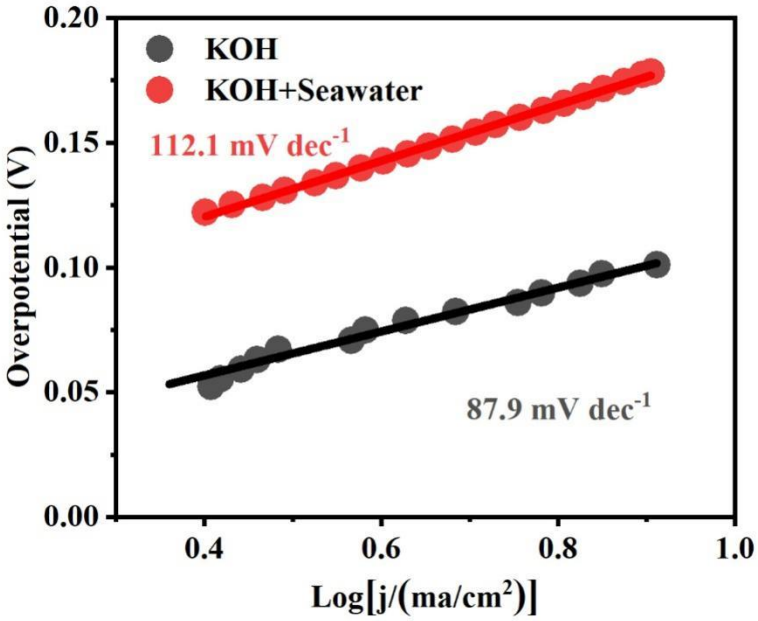

Figure S12. Tafel plots of NiCrS in 1 M KOH + Seawater

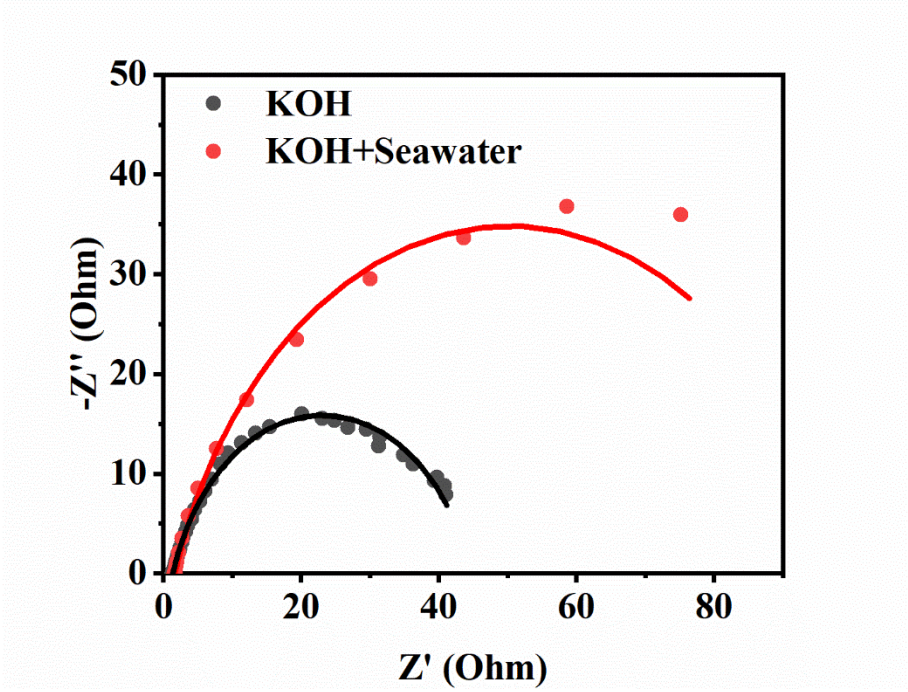

Figure S13. Nyquist diagram of NiCrS in 1 M KOH and 1 M KOH + Seawater

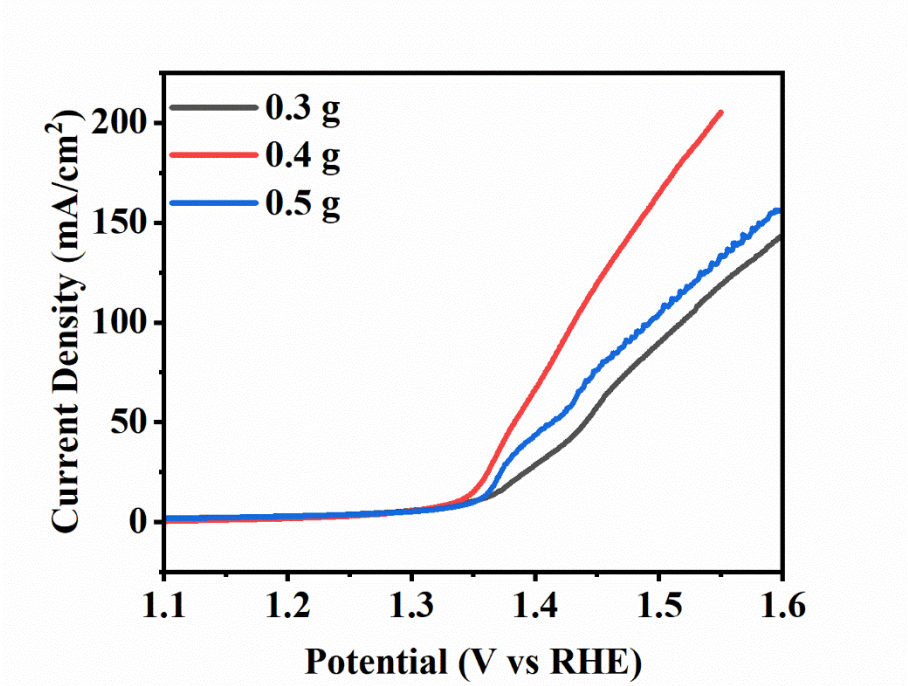

Figure S14. OER polarization curves of NiCrS/CN under different thiourea amounts

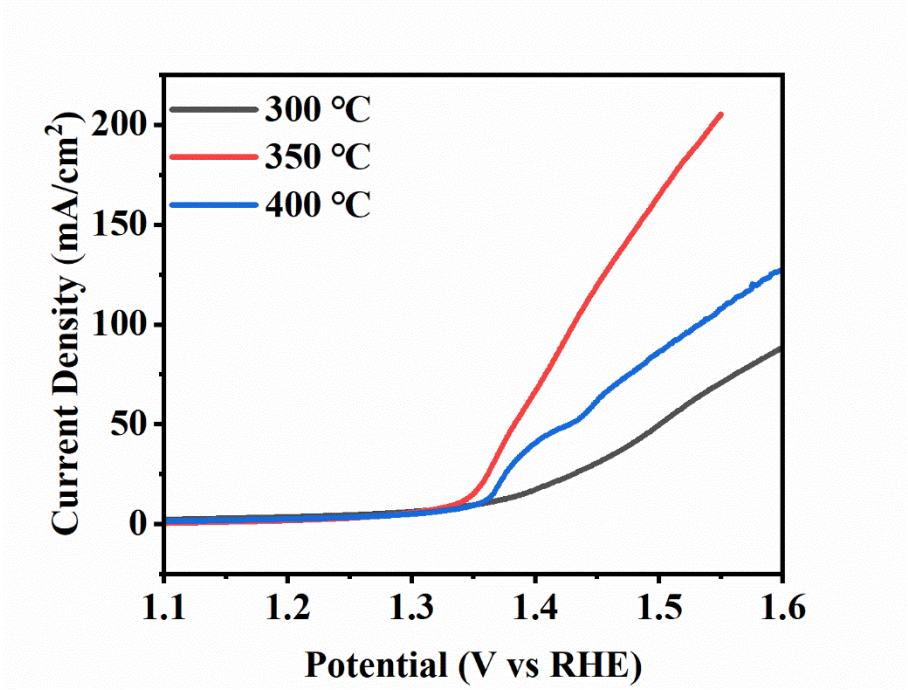

Figure S15. OER polarization curves of NiCrS/CN at different temperatures

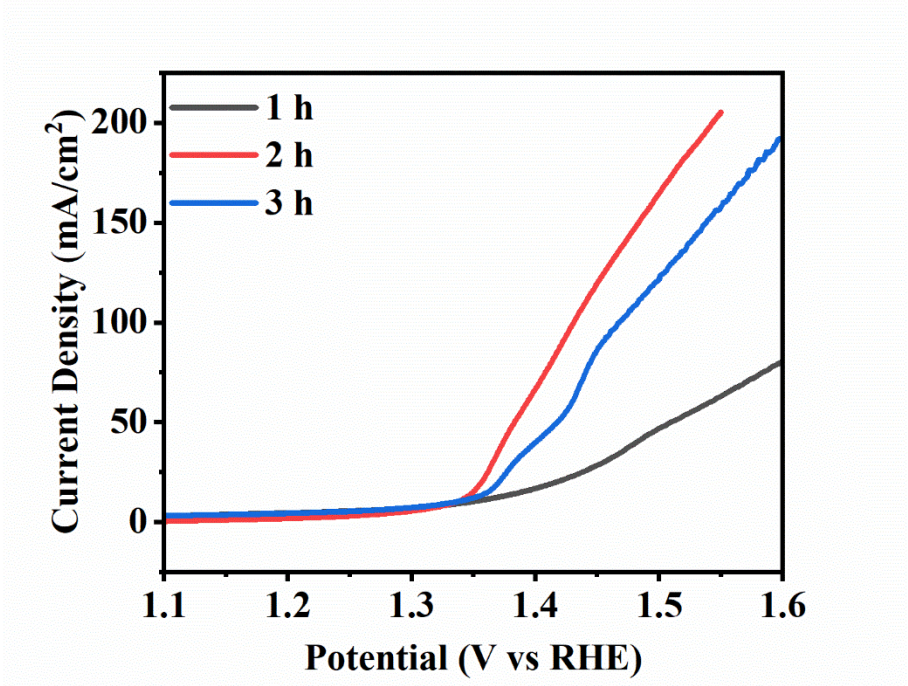

Figure S16. OER polarization curves of NiCrS/CN under different times

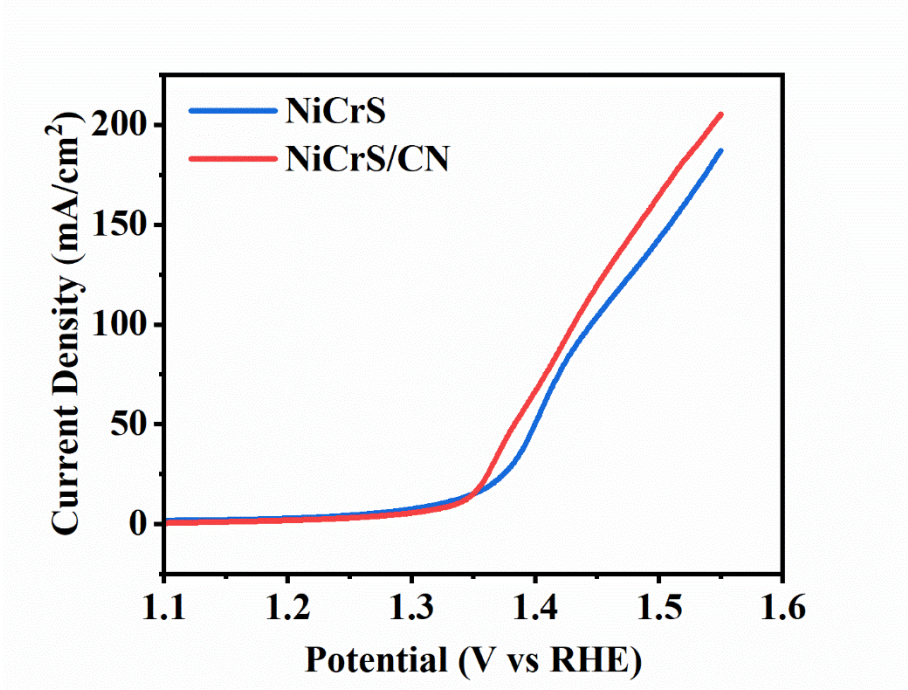

Figure S17. OER polarization curves of NiCrS and NiCrS/CN in 1 M KOH

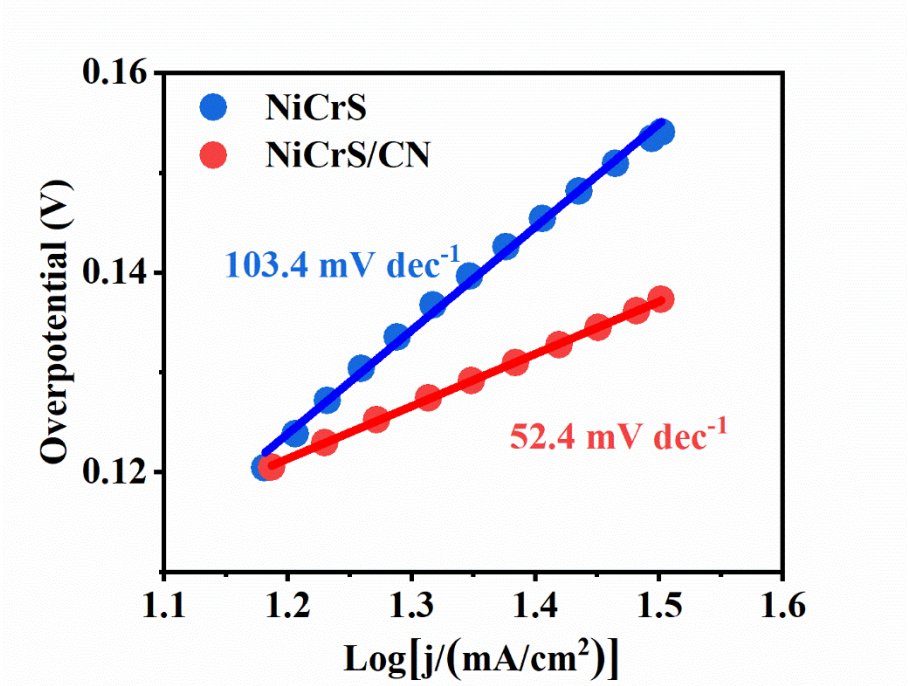

Figure S18. Tafel plots of NiCrS and NiCrS/CN in 1 M KOH

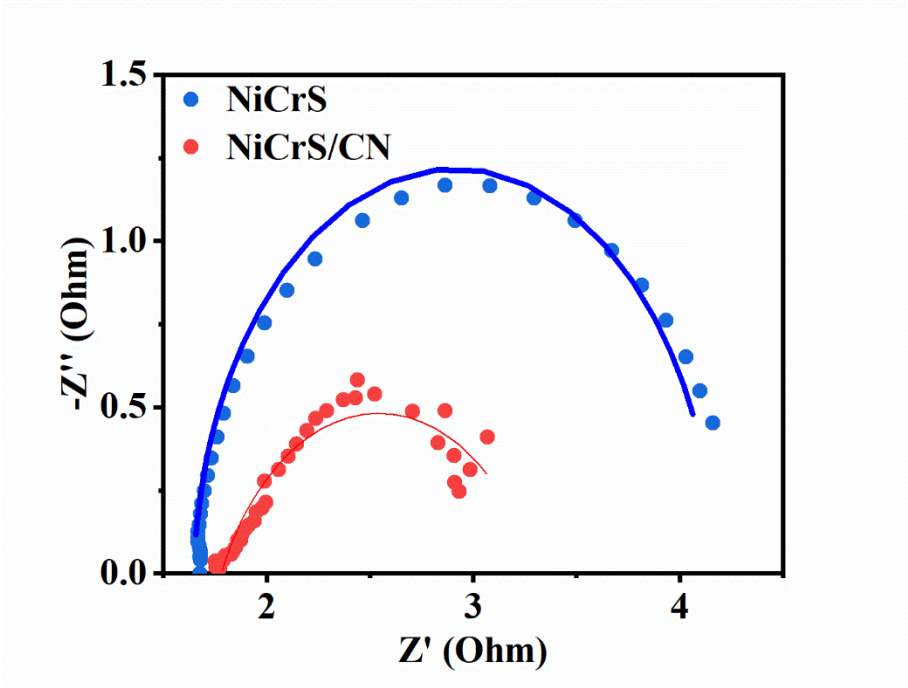

Figure S19. Nyquist diagram of NiCrS and NiCrS/CN in 1 M KOH

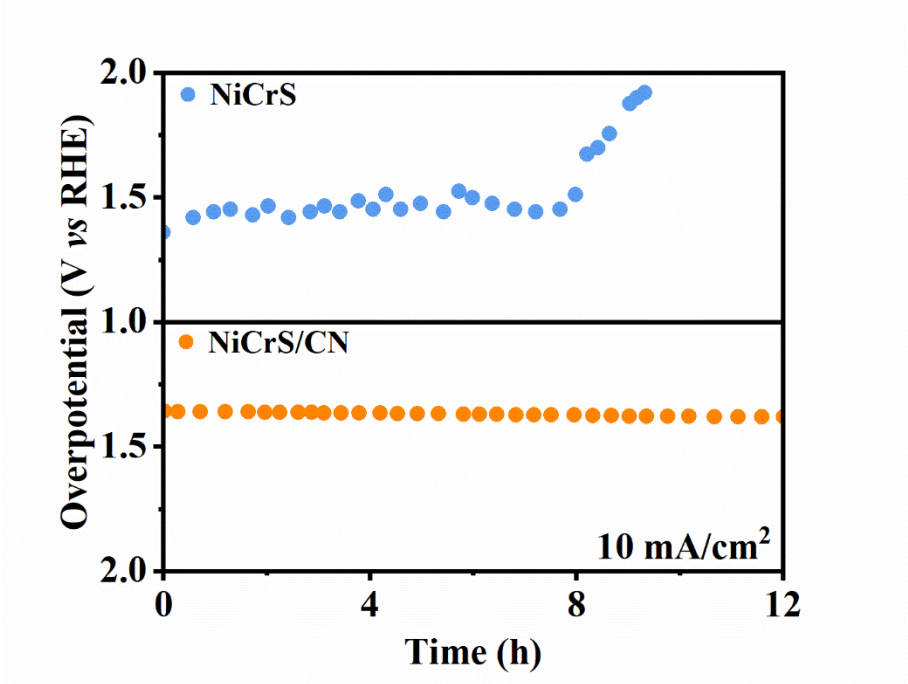

Figure S20. Chronopotential curves of NiCrS and NiCrS/CN in 1 M KOH.

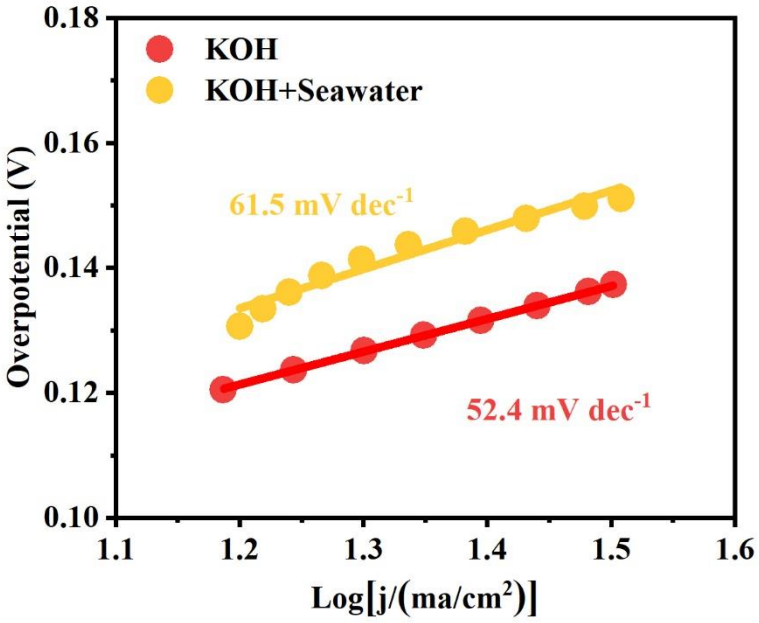

Figure S21. Tafel plots of NiCrS/CN in 1 M KOH and 1 M KOH + Seawater

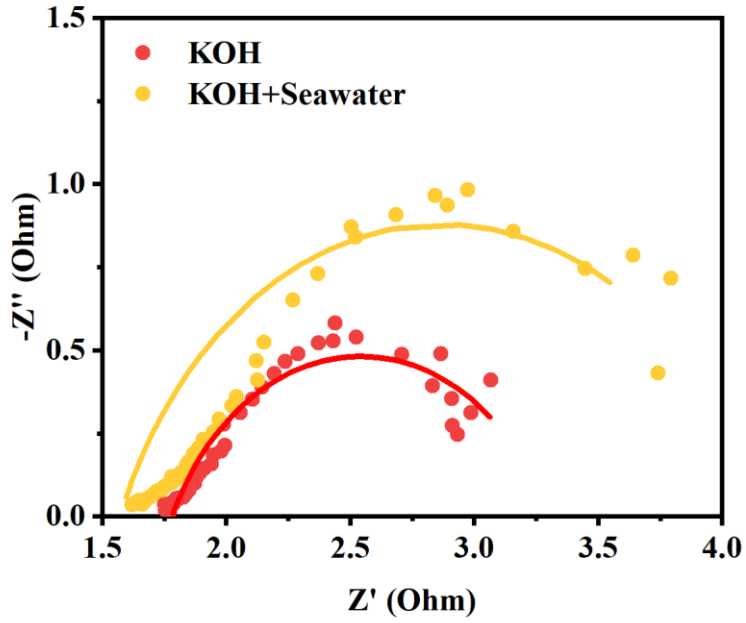

Figure S22. Nyquist diagram of NiCrS/CN in 1 M KOH and 1 M KOH + Seawater.

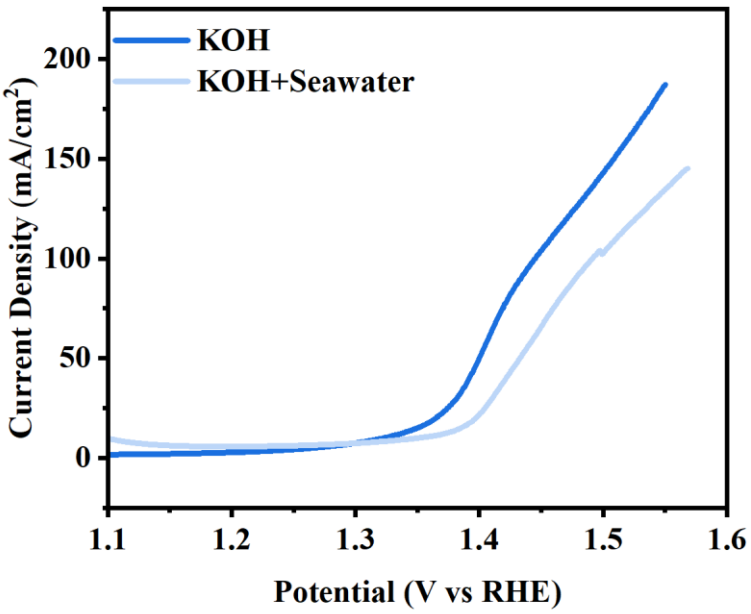

Figure S23. LSV curves of NiCrS for OER in 1 M KOH and 1 M KOH + Seawater.

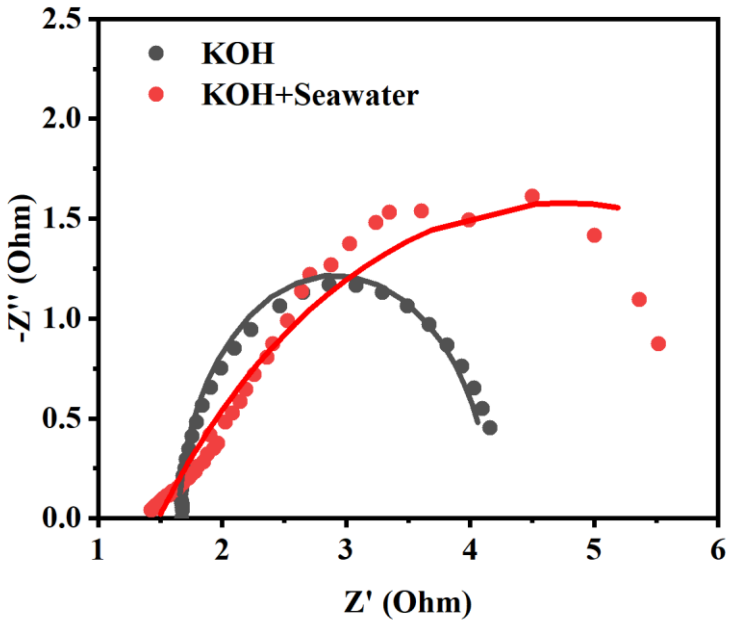

Figure S24. Nyquist diagram of NiCrS in 1 M KOH and 1 M KOH + Seawater.

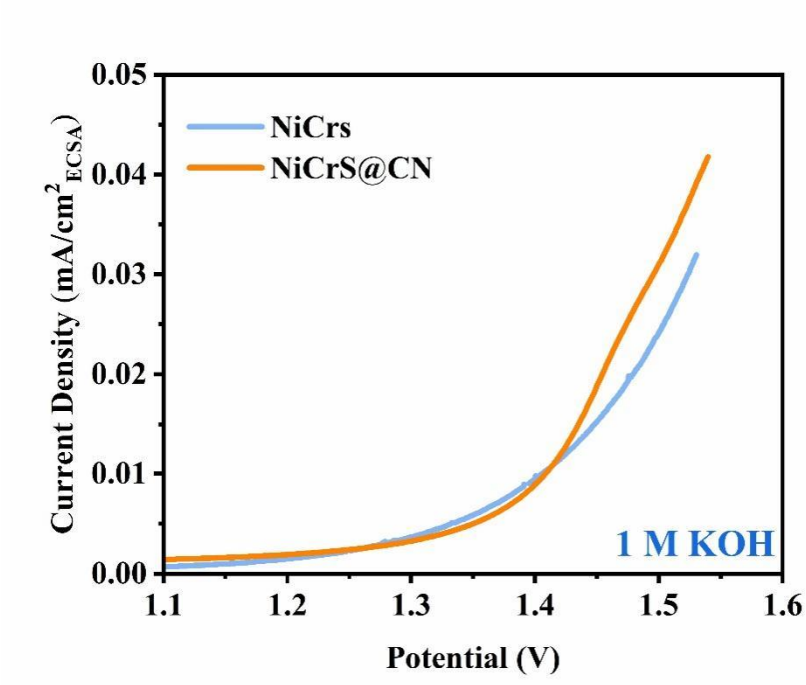

Figure S25. ECSA normalized LSV curves of NiCrS and NiCrS/CN for overall water splitting in 1 M KOH in two electrode configuration

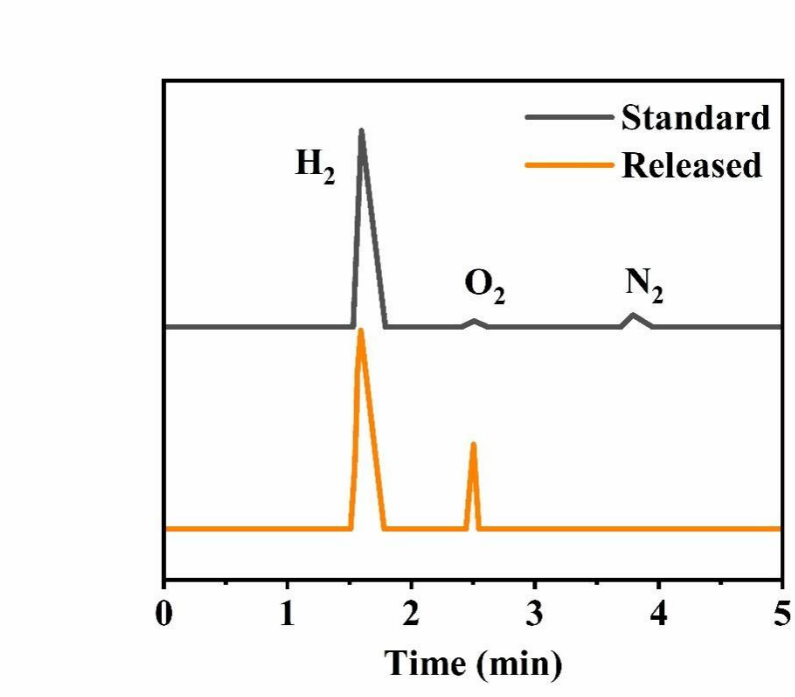

Figure S26. GC results of NiCrS@CN for water splitting in 1 M KOH + Seawater

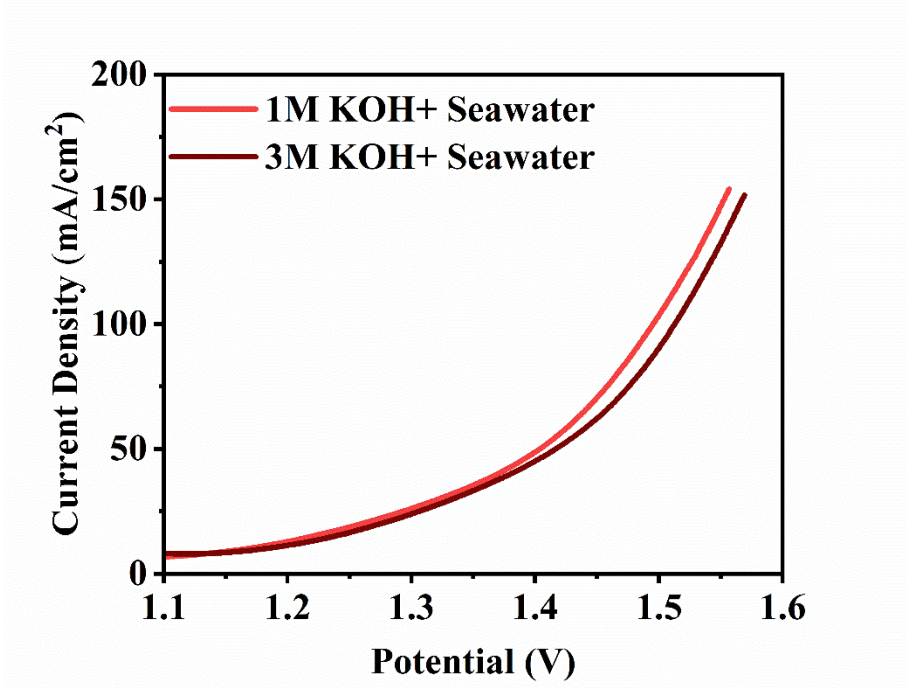

Figure S27. LSV curves of NiCrS@CN for water splitting in 1 M KOH + Seawater and 3 M KOH + Seawater

Table S1. Comparison of electrocatalytic HER activities of various nonprecious catalysts reported in the literature

Catalyst	Electrolyte	J (mA cm^{-2})	η (mV)	Reference
NiCrS/CN	1.0 M KOH + Seawater	10	108	This work
Ni-SN@C	1.0 M KOH + Seawater	10	23	Adv. Mater. 2021, 33, 2007508.
P-Fe7S8@Co9S8@ Ni3S2/NF	1.0 M KOH + 0.5 M NaCl	10	89	Int. J. Hydrogen Energ., 2025, 103: 174-182.
MoN-Co2N	1.0 M KOH + Seawater	10	105	ACS Appl. Mater. Interfaces 2022, 14, 37, 41924–41933
(NiFeCoV)S2	1.0 M KOH + Seawater	10	110	J. Colloid. Interf. Sci., 2023, 645: 724-734.

CoPx	1.0 M KOH + Seawater	10	117	Appl. Catal. B-Environ. Energy, 2021, 294: 120256.
RuW/NCN	1.0 M KOH + Seawater	10	119	J. Colloid. Interf. Sci., 2023, 651: 686-695.
Ni2P-Fe2P/NF	1.0 M KOH + Seawater	10	120	Adv. Funct. Mater. 2021, 31, 2006484.
S&Co-Cu3PNWs/CF	1.0 M KOH + Seawater	10	127.2	J Porous Mater 2021, 28, 763–771
CoSe2-NCF	1.0 M KOH + Seawater	10	134	Inorg. Chem. Commun., 2022, 146: 110170.
(Co,Fe)PO4	1.0 M KOH + Seawater	10	137	NANOMATERIALS-BASEL. 2021, 11, 2989.
Ni-SA/NC	1.0 M KOH + Seawater	10	139	Adv. Mater.2021, 33, 2003846
Mo-Ni2P/CC	1.0 M KOH + Seawater	10	154	New J. Chem., 2022,46, 20602-20609
MFC-2	1.0 M KOH + Seawater	10	154	J. Mater. Chem. A 2023, 11 (23), 12151-12163.
NiSe2	1.0 M KOH + Seawater	10	154.5	Mater. Res. Bull., 2025, 189: 113463.
CoFe-LDH/NF	1.0 M KOH + Seawater	10	159	J. Colloid. Interf. Sci., 2021, 604, 767-775.
NiMoN@NC	1.0 M KOH + Seawater	10	164	Acta Chim. Sin. 2022, 80 (10), 1394-1400.
FeNiP-NPHC	1.0 M KOH + Seawater	10	180	Adv. Funct. Mater., 2022, 32, 2205767.
NiFe-LDH@Ni3S2	1.0 M KOH + Seawater	10	197	Electrochim. Acta, 2019, 318, 42-50.

NFP@NC	1.0 M KOH + Seawater	10	206	Sci. China Mater., 2023, 66 (12), 4630-4638.
Co−P/NF	1.0 M KOH + Seawater	10	213	Eur. J. Inorg. Chem., 2023, 26, e202200657.
Co/Co3O4@C	1.0 M KOH + Seawater	10	357	Int. J. Hydrogen Energy 2020, 45, 33028–33036

Table S2. Comparison of electrocatalytic OER activities of various nonprecious catalysts reported in the literature

Catalyst	**Electrolyte**	**J (mA cm^{-2})**	**η (mV)**	**Reference**
NiCrS/CN	1.0 M KOH + Seawater	10 100	108 200	This work
$NiSe_2$	1.0 M KOH + Seawater	10	183.5	10.1016/j.materresbull.2025.113463
Co-Ni-S/NF	1.0 M KOH + 0.5 M NaCl	100	340	https://doi.org/10.1016/j.jallcom.2023.171124
$CoB_{0.8}$	1.0 M KOH + Seawater	10	232	https://doi.org/10.1039/D5CC03562G
Mn-Ni_3S_2 @Co_9S_8/NF	1.0 M KOH + Seawater	10	261	Fuel, 2024, 377, 132781.
Ag@NiCo	1.0 M KOH + 0.5 M NaCl	10	269	ACS Appl. Energy Mater., 2025, 8, 3416-3424
FCDs/FeCoSe-VSe/NF	1.0 M KOH + Seawater	10	297	Appl. Surf. Sci., 2025, 680, 161456.
$FeSe_2$/$Ni_{0.85}$Se	1.0 M KOH + 0.5 M NaCl	10	267	Int. J. Hydrogen Energy, 2025, 97, 632-639.
FeCoNiMnMo	1 M KOH + simulated seawater	10	237	J. Mater. Sci. Technol., 2023, 138, 29-35.
$CNWFVO_x$	1.0 M KOH + 0.5	10	272	Int. J. Hydrogen Energy,

	M NaCl			2023, 48, 26729-26739.
CSC-Fe	1 M KOH + simulated seawater	10	359	J. Power Sources, 2024, 614, 235017.
NFP@NC	1.0 M KOH + Seawater	10	280	Sci. China Mater., 2023, 66, 4630-4638
20-Fe-NiSe	1.0 M KOH + 0.5 M NaCl	10	311	Mater. Today Chem., 2024, 40, 102276.